Supplementary Information for

Probing foams from the nanometer to the millimeter by coupling small-angle neutron scattering, imaging, and electrical conductivity measurements.

Julien Lamolinairie[1], Benjamin Dollet[2], Jean-Luc Bridot[3], Pierre Bauduin[4], Olivier Diat[4], and Leonardo Chiappisi[1]

[1]Institut Max von Laue - Paul Langevin (ILL), 71 avenue des Martyrs, 38042 Grenoble, France
[2]Université Grenoble Alpes, CNRS, LIPhy, 38000 Grenoble, France
[3]Teclis Scientific, 69380 Civrieux-d'Azergues, France
[4]ICSM, Univ Montpellier, CEA, CNRS, ENSCM, Marcoule, France

S1 Materials

The densities and scattering length densities (SLD) for all the chemicals used are given in Table 1.

Coumpound	Density (g.cm^{-3})	SLD (Å^{-2})	v(Å^3)
D_2O	1.1	$6.33 \cdot 10^{-6}$	-
$C_{18}E_{10}$	0.95	$7.73 \cdot 10^{-8}$	-
C18:1	0.85	$-1.75 \cdot 10^{-7}$	520
E10	1.19	$6.00 \cdot 10^{-7}$	610

Table S1: Densities, scattering length densities (SLD) and volumes v for the compounds used in this work.

S2 Image processing

S2.1 Thresholding

The adaptive thresholding is the method where the threshold value is calculated for small regions in pictures. This leads to different threshold values for different regions with respect to the change in lighting. We use *cv2.ADAPTIVE THRESH MEAN* method where threshold Value of a given pixel is calculated as the mean of the neighbourhood area values – constant value). In other words, it is the mean of the blockSize×blockSize neighborhood of a point minus a chosen constant.

```
import cv2   #install opencv-python

def load_and_convert_image(input_image):
    # Reading image and converting it to gray scale
    img = cv2.imread(input_image)
    gray_img = cv2.cvtColor(img, cv2.COLOR_BGR2GRAY)

    # Get a blank canvas for drawing contour
    canvas = np.zeros(gray_img.shape, np.uint8)

    # Applying thresholding technique on the gray image
```

```
    th = cv2.adaptiveThreshold(gray_img, 255, cv2.ADAPTIVE_THRESH_MEAN_C, cv2.
    THRESH_BINARY_INV, 55, 5) #blockSize = 55 and constant = 5
    th = cv2.bitwise_not(th2)

    # Applying a contour detection to remove impurities
    contours, hierarchy = cv2.findContours(th2,cv2.RETR_TREE,cv2.CHAIN_APPROX_SIMPLE)
    for cnt in contours:
        cv2.drawContours(th2,[cnt],0,255,-1)
    img_final = cv2.bitwise_not(th)
    img_final = cv2.bitwise_not(img_final)

    cv2.waitKey(0)

    return img_final
```

Listing 1: Python code used for image thresholding

S2.2 Skeletonize function

This process involves repeatedly removing pixels from the edges of objects in a binary image until they are reduced to single-pixel-wide shapes. This command is applied directly to the previously binarised images, as shown in Fig. S1d.

```
def skeleton(img_final):
    # Step 1: Create an empty skeleton
    size = np.size(img_final)
    skel = np.zeros(img_final.shape, np.uint8)
    img_final = cv2.bitwise_not(img_final)
    # Get a Cross Shaped Kernel
    element = cv2.getStructuringElement(cv2.MORPH_CROSS, (3,3))

    # Repeat steps 2-4
    while True:
        #Step 2: Open the image
        open = cv2.morphologyEx(img_final, cv2.MORPH_OPEN, element)
        #Step 3: Substract open from the original image
        temp = cv2.subtract(img_final, open)
        #Step 4: Erode the original image and refine the skeleton
        eroded = cv2.erode(img_final, element)
        skel = cv2.bitwise_or(skel,temp)
        img_final = eroded.copy()
        # Step 5: If there are no white pixels left ie.. the image has been
    completely eroded, quit the loop
        if cv2.countNonZero(img_final)==0:
            break

    cv2.waitKey(0)
    #cv2.destroyAllWindows()

    return skel
```

Listing 2: Python code used for image skeletonization

S2.3 Measurement of the Plateau border radius

The images taken through the prism with the telecentric lens have the following advantage. Because the rays of light are refracted as soon as they cross an air/liquid interface with is not parallel to the cell walls, the thickness of the Plateau borders in contact with the cell walls is equal to twice the radius of the Plateau borders r_{PB}.

Hence, to measure r_{PB}, we propose the following simple method. First, we measure the distance map of the binarised images, i.e. the distance of each "black" pixel (inside a Plateau border) from the closest bubble. Second, we turn to the skeletonized image: since the skeleton passes through the midline of the Plateau borders between neighbouring bubbles, we record the distance from the distance

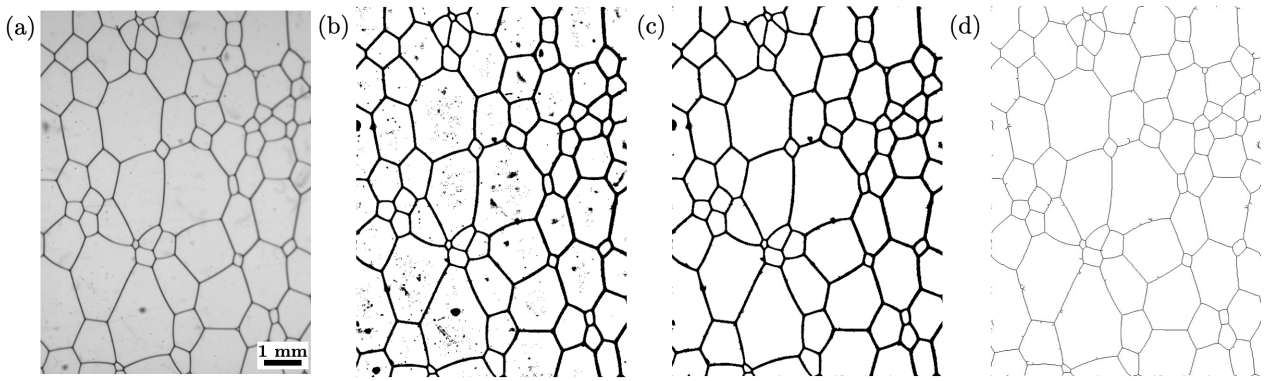

Figure S1: **(a)** Image of a foam before any processing, **(b)** after binarisation, **(c)** after contour filling and **(d)** after topological skeleton process.

map of each pixel pertaining to the skeleton, and we define r_{PB} as the average of all these individual distances. An illustration of the different steps is given in Fig. S2.

A limitation of this method is that some of the pixels pertaining to the skeleton are not part of Plateau borders, but of vertices, which are thicker. For such pixels, this leads to an overestimation of r_{PB} (see Fig. S2c). This may affect the images at short times, when the foam is the wettest. However, the method is very reliable for dry foams. It is also worth noticing that the limitation due to spatial resolution is compensated by the averaging over a large number (of order 10^4, in our experiments) of skeleton pixels, which increases the precision of the measurement of r_{PB}.

S3 Micelle analysis with SANS

The analytical expression used to describe the scattering patterns of polyoxyethylene alkyl ether carboxylic acid were published in earlier manuscripts[1, 2, 3, 4] and are reported here for the sake of completeness. In all cases, a core-shell structure was considered, with an anhydrous core composed by the surfactant alkyl chains while the hydrated shell contains the EO units, the carboxymethyl termination and hydration water. The scattering length density of the shell is calculated as the volume weighted average of solvent and surfactant headgroup.

S3.1 Surfactant globular micelles

The globular micelles were described using the form factor of core-shell ellipsoids[5] $P_{CS}(q)$ and a structure factor for charged hard spheres $S_{\mathrm{cHS}}(q)$ including the hard sphere and electrostatic repulsion treated in the random phase approximation (RPA)[6]. The particle number density ${}^1N$ was calculated from the micellar core as:

$$ {}^1N = \frac{3\phi^{\mathrm{core}}}{4\pi AB^2} \tag{S1}$$

with ϕ^{core} being the volume fraction of the core, A and B being the rotational and equatorial semi-axes of the ellipsoidal core, respectively. The volume fraction of the core is expressed as

$$ \phi^{\mathrm{core}} = \frac{v_c}{v_c + v_s}\phi_{\mathrm{Brij}} + \phi_{\mathrm{SDS}} \tag{S2}$$

with ϕ_{Brij} the volume fraction of BrijO10 and ϕ_{SDS} of SDS; v_c the volume of apolar part and v_s of polar part of BrijO10. It was assumed that SDS is contained only in the core due to its small head. The fraction of SDS in the core is then expressed as

$$ \phi^{\mathrm{core}}_{SDS} = \frac{V^{\mathrm{core}}_{\mathrm{SDS}}}{V^{\mathrm{core}}_{\mathrm{SDS}} + V^{\mathrm{core}}_{\mathrm{BrijO10}}} = \frac{1}{1 + R\frac{v_c}{v_{c,SDS}}} \tag{S3}$$

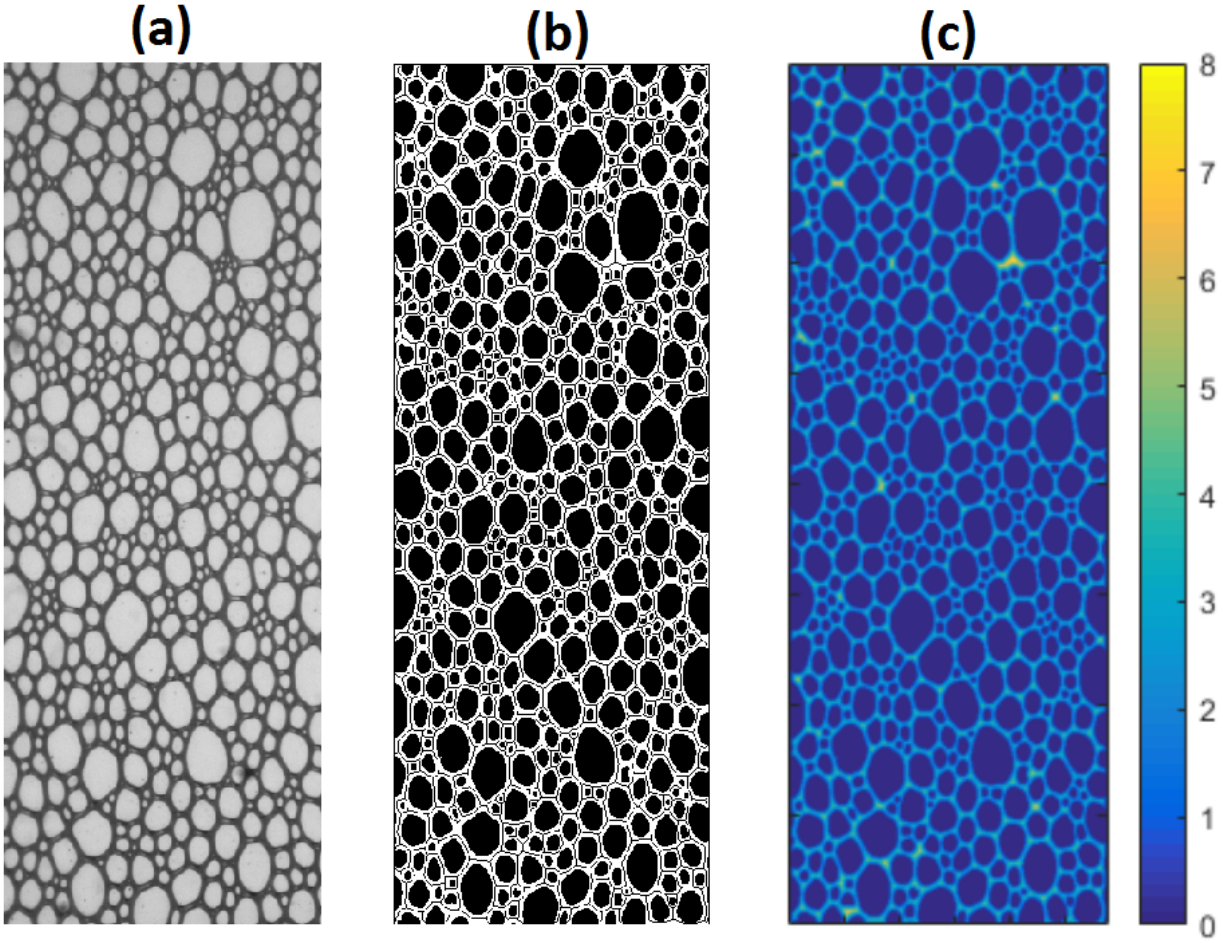

Figure S2: Illustration of the measurement of the Plateau border radius, here on an extract of an image of the foam at $t = 9$ min (see also Fig. S5). (a) Raw image, (b) Binarised version of image (a), where the interior of the bubbles appear in black and the wall Plateau borders in white, overlaid with the skeletonisation of the Plateau borders (the skeleton is constituted by the one-pixel-thick lines in the middle of the Plateau borders. (c) Distance map from the interior of the bubbles (here in dark blue): the colours in the Plateau borders correspond to the distance to the closest bubble (the colour bar on the right indicates the correspondence between colour and distance in pixels).

with R the ratio of surfactants between BrijO10 and SDS, and $v_{c,SDS}$ the volume of apolar part of SDS. The scattering intensity using the monodisperse centro-symmetric approximation is given by:

$$I(q) = {}^1N P_{CS}(q) S_{\mathrm{cHS}}(q) \tag{S4}$$

S3.1.1 Scattering form factor

The isotropically averaged scattering form factor is given by[7]:

$$P_{CS}(q) = \int_0^1 |F(q, \cos\alpha)|^2 \mathrm{d}\cos\alpha \tag{S5}$$

with α being the angle formed by the scattering vector and the rotational axis of the ellipsoid. $F(q, \cos\alpha)$ is the scattering amplitude and is given by

$$F(q, \cos\alpha) = (\mathrm{SLD_c} - \mathrm{SLD_{sh}})\, V_c \left[\frac{3j_1(x_c)}{x_c}\right] + \left(\mathrm{SLD_{sh}} - \overline{\mathrm{SLD}}\right) V_t \left[\frac{3j_1(x_t)}{x_t}\right] \tag{S6}$$

with $\mathrm{SLD_{sh}}$ and $\overline{\mathrm{SLD}}$ being the scattering length densities of the micellar shell and of the medium, respectively. Core $\mathrm{SLD_c}$ is approximated by the SLD of C18:1 as BrijO10 is in excess compared to

SDS. Moreover, the chain length is almost identical for the two surfactants (12 carbons for SDS and 18 for BrijO10) The scattering length density of the shell was obtained as the volume average of the SLDs of the hydrophylic part of the surfactant and the solvent. $j_1(x)$ is the first order spherical Bessel function:

$$j_1(x) = \frac{\sin(x) - x\cos(x)}{x^2} \tag{S7}$$

x_c and x_t are given by:

$$x_c = q\sqrt{A^2\cos^2\alpha + B^2(1-\cos^2\alpha)} \tag{S8}$$

$$x_t = q\sqrt{(A+T)^2\cos^2\alpha + (B+T)^2(1-\cos^2\alpha)} \tag{S9}$$

and the volumes of the core and of the particle are

$$V_c = \frac{4}{3}\pi AB^2 \tag{S10}$$

$$V_t = \frac{4}{3}\pi(A+T)(B+T)^2 \tag{S11}$$

The water content of the shell was calculated as

$$\phi_w^{\text{shell}} = \frac{V_{\text{sh}} - N_{\text{agg}}^{\text{BrijO10}} v_s}{V_{\text{sh}}} \tag{S12}$$

with $V_{sh} = V_t - V_c$ being the volume of the hydrated shell and v_s the average volume of the surfactant headgroup. The aggregation number (number of BrijO10 and SDS per micelle) are calculated as:

$$N_{\text{agg}}^{\text{BrijO10}} = \frac{V_{\text{core}}}{v_c}\left(1 - \phi_{SDS}^{\text{core}}\right) \quad \text{and} \quad N_{\text{agg}}^{\text{SDS}} = \frac{V_{\text{core}}}{v_{c,SDS}}\phi_{SDS}^{\text{core}} \tag{S13}$$

S3.1.2 Scattering structure factor

A scattering structure factor of repulsive hard spheres was used to account for the interparticle interactions among globular micelles and is given by:[6]

$$S_{\text{cHS}}(q) = \left[1 - {}^1N\left(C_0(q) - \frac{U(q)}{k_BT}\right)\right]^{-1} \tag{S14}$$

with ${}^1N$ the number density of colloids, $k_B = 1.381 \cdot 10^{-23}$ N m K^{-1} the Boltzmann constant and T the temperature in kelvin. The hard sphere repulsion is expressed as:

$$\begin{aligned} {}^1NC_0(q) = \frac{A}{x^3}(\sin x - x\cos x) + \frac{B}{x^3}\left(\left(\frac{2}{x^2} - 1\right)x\cos x + 2\sin x - \frac{2}{x}\right) \\ - \frac{A\phi_{HS}}{2x^3}\left[\frac{24}{x^3} + 4\left(1 - \frac{6}{x^2}\right)\sin x - \left(1 - \frac{12}{x^2} + \frac{24}{x^4}\right)x\cos x\right] \end{aligned} \tag{S15}$$

with $x = 2R_{HS}q$, $A = -24\phi_{HS}\left(\frac{1+2\phi_{HS}}{(1-\phi_{HS})^2}\right)^2$ and $B = 36\left(\phi_{HS}\frac{2+\phi_{HS}}{(1-\phi_{HS})^2}\right)^2$. The charge perturbation is written as the result from the DLVO theory for distances greater than the hard sphere radius, giving:

$$\frac{{}^1NU(q)}{k_BT} = 4\frac{e_0^2}{k_B\epsilon_0}\frac{{}^1N}{\epsilon_r T}\left(\frac{R_{HS}Z}{2+s}\right)^2\frac{x\cos x + s\sin x}{x\left(x^2+s^2\right)} \tag{S16}$$

where $s = 2\kappa R_{HS}$, $\kappa^{-1} = \sqrt{\epsilon_0\epsilon_r k_BT/2N_AIe_0^2}$ is the Debye length, N_A the Avogadro constant, e_0 the elementary charge, ϵ_0 the dielectric constant and ϵ_r the relative static permittivity of the solvent, Z is the effective number of charges per colloid. The ionic strength is calculated as

$$I = \frac{1}{2}\sum_i c_i z_i = \frac{1}{2}[Na^+] = \frac{1}{2}[SDS] = 1 \cdot 10^{-4}\ M \tag{S17}$$

assuming that only the counter ion Na^+ from SDS contribute to the ionic strength. The effective surface potential is given by:

$$\psi_0 = Ze_0/\left[2\pi R_S\epsilon_0\epsilon_r(2+s)\right]. \tag{S18}$$

The data and the fit are shown in Fig. S3 and Table S2.

A	B	T	R_{HS}	ϕ_w^{shell}	$N_{\text{agg}}^{\text{BrijO10}}$	$N_{\text{agg}}^{\text{SDS}}$	Z
38	22	15	42	68	121	48	12

Table S2: Fit parameters according to the core–shell ellipsoidal model with charged hard-spheres structure factor. The ellipsoidal axes A and B, the shell thickness T as well as the hard sphere radius are given in Å and the water content of the shell ϕ_w^{shell} is given in %.

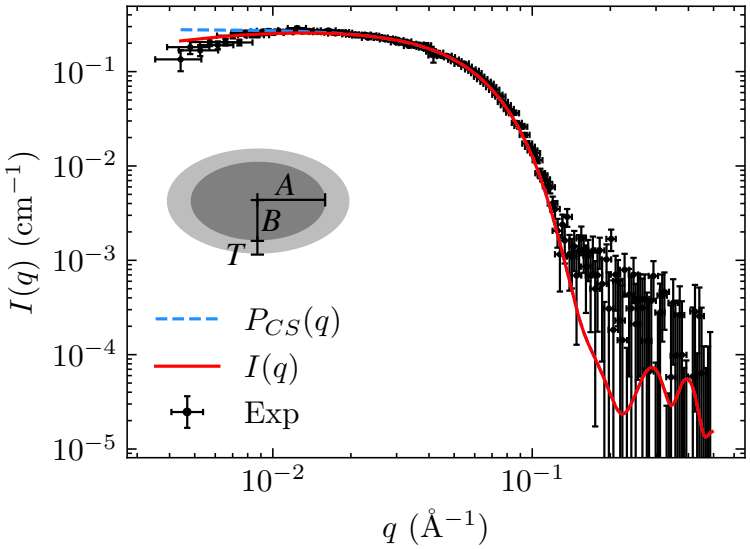

Figure S3: SANS data for the micellar solution. Red straight line corresponds to the fit of the intensity $I(q)$ and the blue dotted line corresponds to the form factor $P_{CS}(q)$. A representation of core-shell model is included in the graph.

S4 Foam analysis with SANS

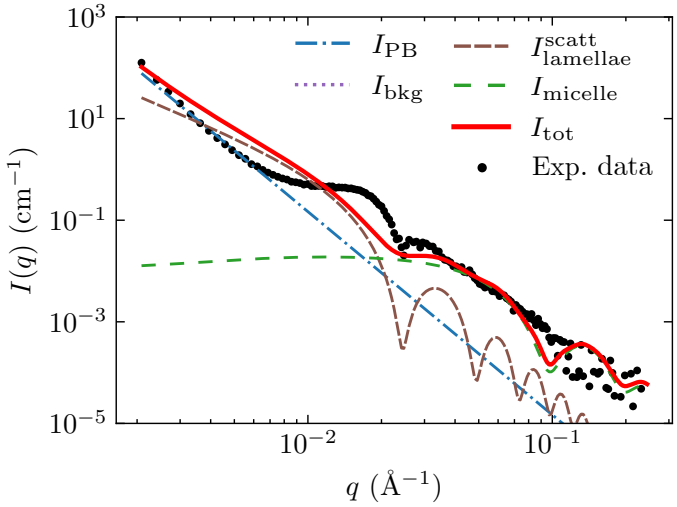

Figure S4: Experimental SANS data recorded at 65 min after stopping foaming and calculated contributions to the overall signal: I_{PB} from Plateau borders, I_{micelle} from micelles present within the foam and $I_{\text{lamellae}}^{\text{scatt}}$ considering the scattering contribution from the lamellae. The film thickness obtained is equal to $h = 26$ nm, but the fit does not correctly describe the data.

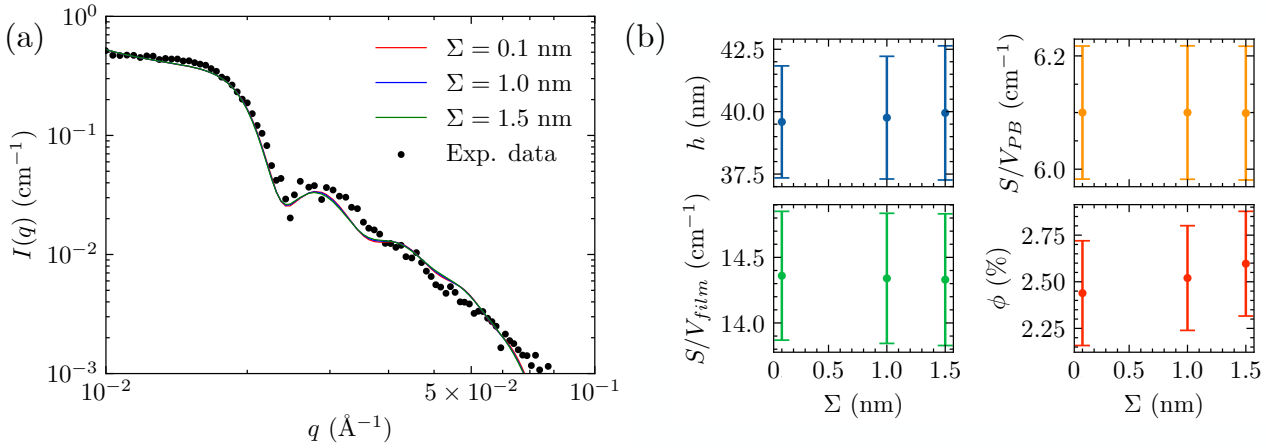

Figure S5: Foam scattering data collected at 65 min of aging to which are superimpose the fitted total intensity for three different values of roughness. The fit parameters and their error bars are shown in Fig. b.

Table S3: Correlation table obtained during the SANS fit procedure of data collected at 65 min of aging.

	h	S/V_{PB}	S/V_{film}	ϕ
h	1			
S/V_{PB}	0.06	1		
S/V_{film}	0.35	0.24	1	
ϕ	0.04	0.01	0.25	1

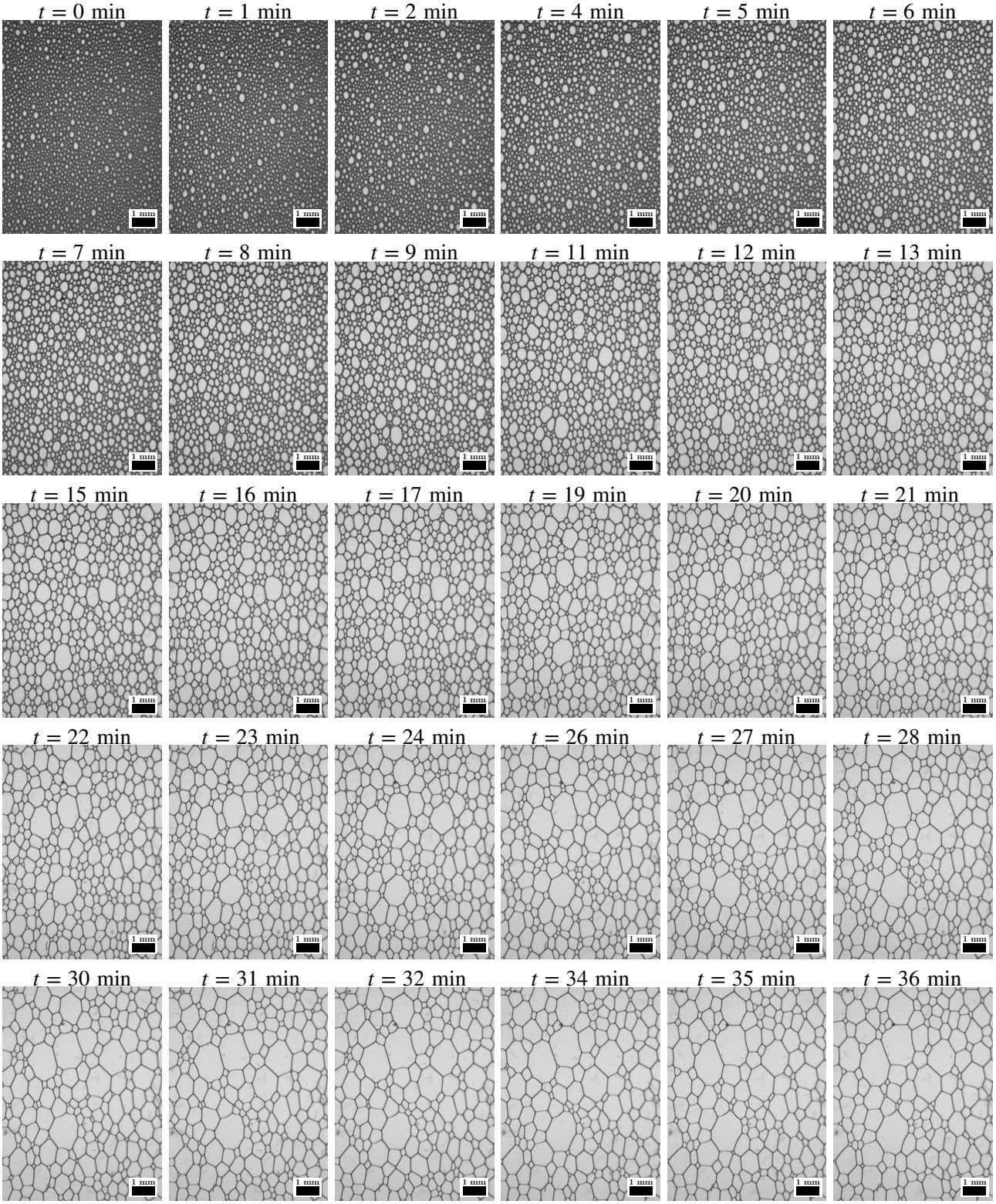
t = 0 min
t = 1 min
t = 2 min
t = 4 min
t = 5 min
t = 6 min
t = 7 min
t = 8 min
t = 9 min
t = 11 min
t = 12 min
t = 13 min
t = 15 min
t = 16 min
t = 17 min
t = 19 min
t = 20 min
t = 21 min
t = 22 min
t = 23 min
t = 24 min
t = 26 min
t = 27 min
t = 28 min
t = 30 min
t = 31 min
t = 32 min
t = 34 min
t = 35 min
t = 36 min
1 mm

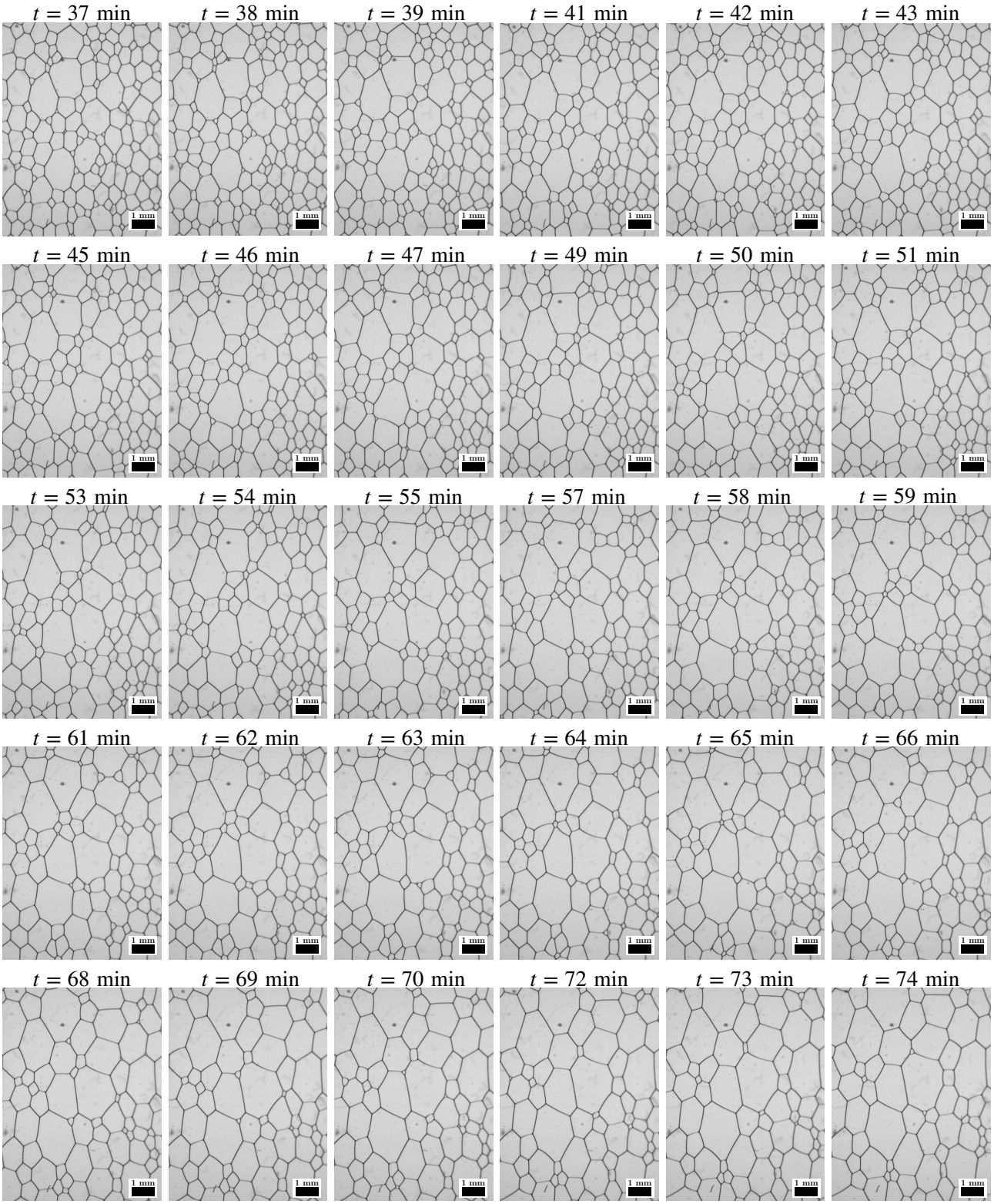

Figure S6: Photographs of the foam under free drainage conditions.

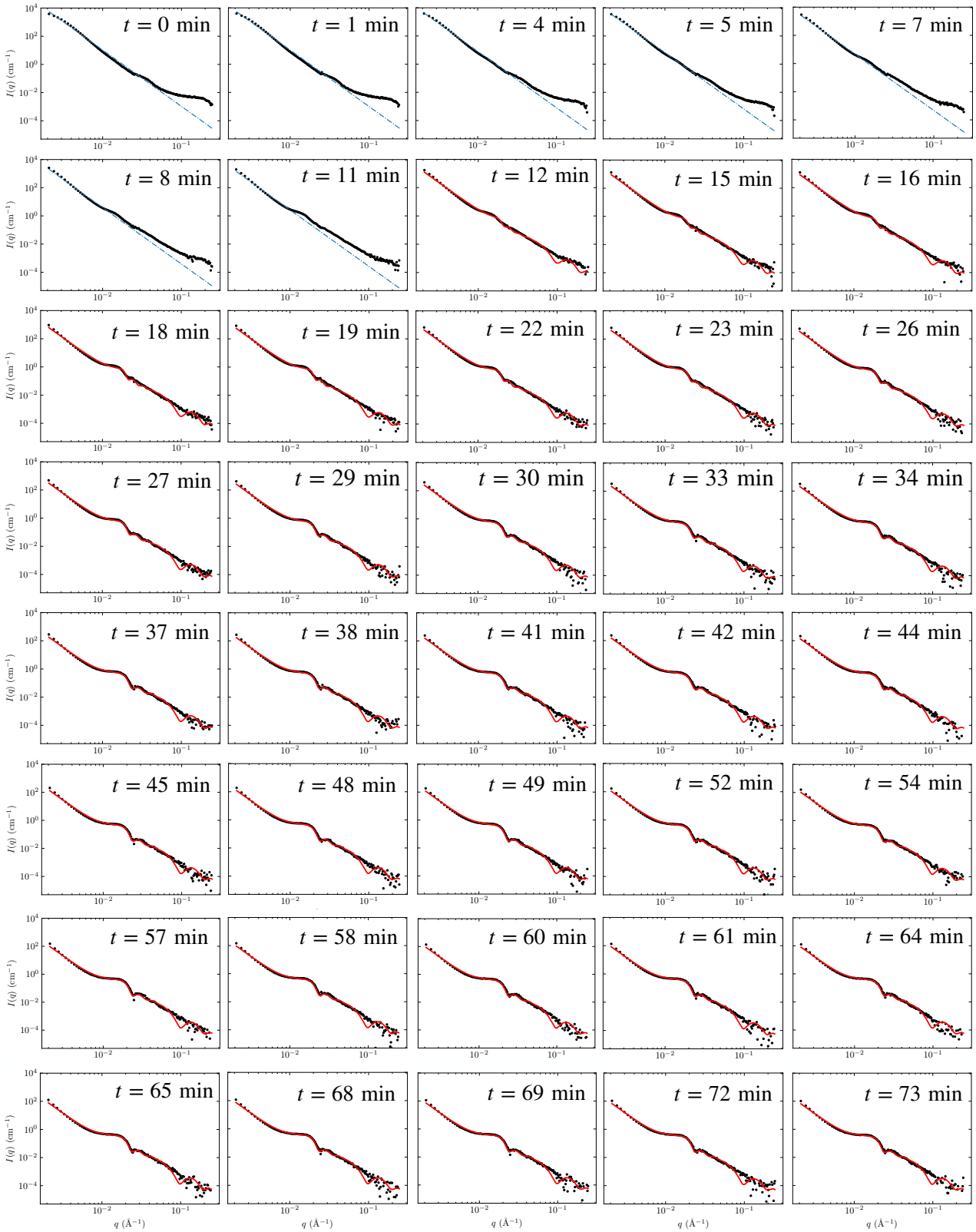

Figure S7: Experimental SANS data (black dot) and the resulting intensity calculated by summing all the contributions. For a time lower 26 minutes, only the contribution of the Plateau Borders (via the Porod law) is represented.

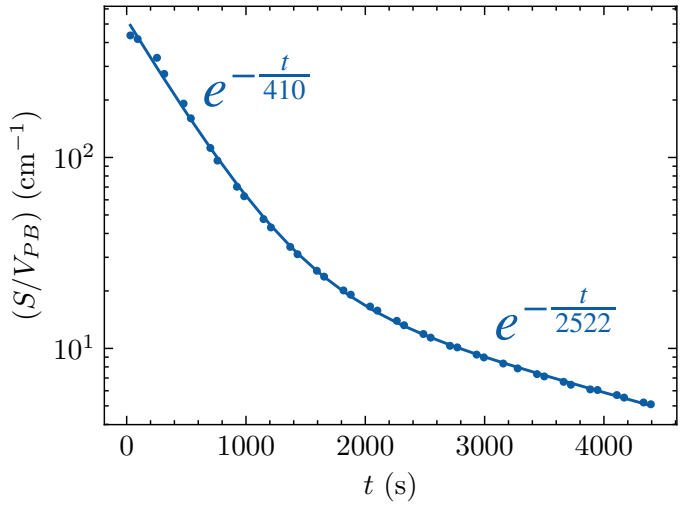

Figure S8: Specific surface area of the Plateau Borders obtained from the SANS data analysis (blue dots). The data are fitted using 2 decaying exponentials represented by the blue lines.

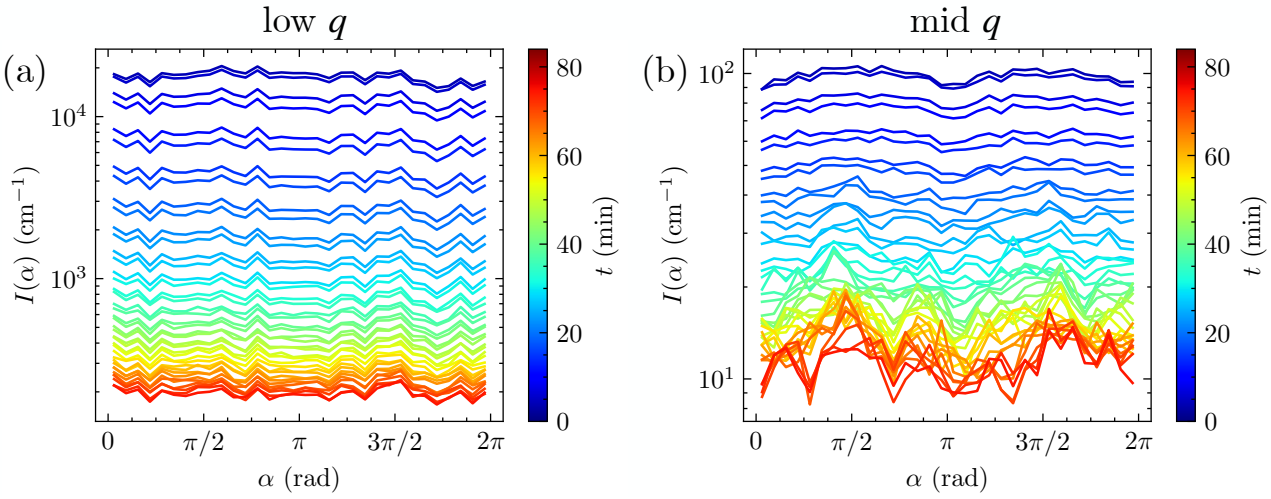

Figure S9: **(a)** Mean intensity for low-q region (q between 0.002 and 0.004 Å^{-1}) and **(b)** mid-q region (q between 0.010 and 0.015 Å^{-1}) as a function of azimuthal angle α and as function of time.

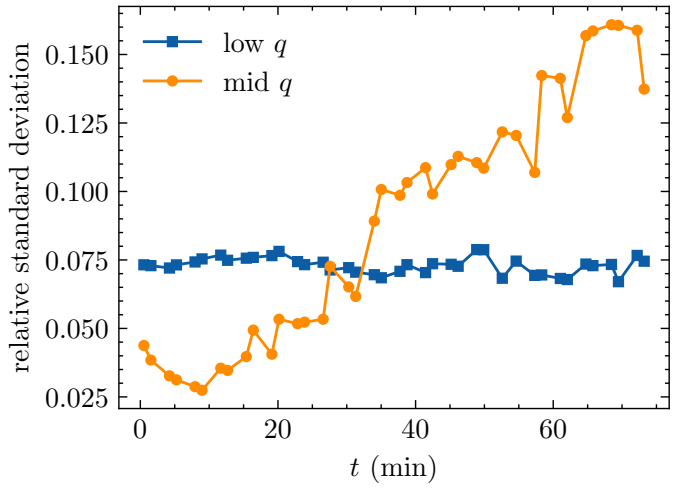

Figure S10: Relative standard deviation of intensity for low-q region (q between 0.002 and 0.004 Å^{-1}) and for mid-q region (q between 0.01 and 0.0150 Å^{-1}).

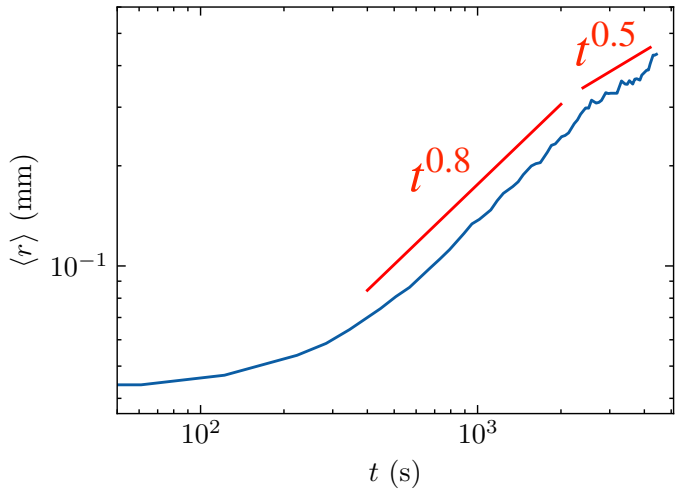

Figure S11: Evolution of the average radius $\langle r \rangle$ and two time laws t^β with $\beta = 0.8$ and $\beta = 0.5$.

References

[1] Leonardo Chiappisi. "Polyoxyethylene alkyl ether carboxylic acids: An overview of a neglected class of surfactants with multiresponsive properties". In: Advances in Colloid and Interface Science 250 (2017), pp. 79–94. ISSN: 0001-8686. DOI: https://doi.org/10.1016/j.cis.2017.10.001. URL: https://www.sciencedirect.com/science/article/pii/S0001868617303561.

[2] Leonardo Chiappisi et al. "From Crab Shells to Smart Systems: Chitosan–Alkylethoxy Carboxylate Complexes". In: Langmuir 30.35 (2014), pp. 10608–10616. DOI: 10.1021/la502569p.

[3] Leonardo Chiappisi et al. "Chitosan/Alkylethoxy Carboxylates: A Surprising Variety of Structures". In: Langmuir 30.7 (2014), pp. 1778–1787. DOI: 10.1021/la404718e.

[4] Michael Schwarze et al. "Oleylethoxycarboxylate – An efficient surfactant for copper extraction and surfactant recycling via micellar enhanced ultrafiltration". In: Journal of Colloid and Interface Science 421 (2014), pp. 184–190. ISSN: 0021-9797. DOI: https://doi.org/10.1016/j.jcis.2014.01.037.

[5] Dalila Bendedouch and Sow Hsin Chen. "Effect of an attractive potential on the interparticle structure of ionic micelles at high salt concentration". In: The Journal of Physical Chemistry 88.4 (1984), pp. 648–652. DOI: 10.1021/j150648a003.

[6] L. Baba-ahmed, M. Benmouna, and M. J. Grimson. "Elastic Scattering from Charged Colloidal Dispersions". In: Physics and Chemistry of Liquids 16.3 (1987), pp. 235–238. DOI: 10.1080/00319108708078524.

[7] Jan Skov Pedersen. "Modelling of Small-Angle Scattering Data from Colloids and Polymer Systems". In: Neutrons , X-rays and Light : Scattering Methods Applied to Soft Condensed Matter. Ed. by Peter Lindner and Thomas Zemb. Elsevier Science Bv, 2002, pp. 391–420.